Journal of Biomedical Optics

BiomedicalOptics.SPIEDigitalLibrary.org

Different Raman spectral patterns of primary rat pancreatic β cells and insulinoma cells

Qiu-Li Zhou
Xi Rong
Fang Wei
Rui-Qiong Luo
Hong Liu

SPIE.

Journal of Biomedical Optics 20(4), 047001 (April 2015)

Different Raman spectral patterns of primary rat pancreatic β cells and insulinoma cells

Qiu-Li Zhou,[a,†] Xi Rong,[b,†] Fang Wei,[a] Rui-Qiong Luo,[a] and Hong Liu[b,*]
[a]Guangxi Medical University, No. 22 Shuangyong Road, Nanning 530021, China
[b]First Affiliated Hospital of Guangxi Medical University, Department of Geriatric Endocrinology, No. 6 Shuangyong Road, Nanning 530021, China

Abstract. As a noninvasive and label-free analytical technique, Raman spectroscopy has been widely used to study the difference between malignant cells and normal cells. Insulinomas are functional β-cell tumors of pancreatic islet cells. They exhibit many structural and immunohistochemical features in common with normal pancreatic β cells; thus, they are typically difficult to distinguish under the microscope, especially *in vivo*. We investigated insulinoma and primary rat pancreatic β-cell populations using Raman spectroscopy. The details of the optical heterogeneity between these two populations were determined based on different Raman regions primarily involving nucleic acid and protein contents, which are the most distinct cellular contents in these two types of cells. Using principal component analysis–linear discriminant analysis, these two cell types can be readily separated. The results of this work indicate that Raman spectroscopy is a promising tool for the noninvasive and label-free differentiation of insulinoma cells and normal pancreatic β cells. [DOI: 10.1117/1.JBO.20.4.047001]

Keywords: Raman spectra; pancreatic β cell; insulinoma.

Paper 150004PRR received Jan. 4, 2015; accepted for publication Mar. 17, 2015; published online Apr. 7, 2015.

1 Introduction

There is considerable interest in Raman vibrational spectroscopy as a diagnostic tool for rapidly determining the characteristics of different samples. This technique provides a unique opportunity to analyze chemical concentrations in individual cells at the submicrometer length scale without the need for optical labels,[1] thus enabling the rapid and noninvasive assessment of the cellular biochemistry inside living cells and allowing for real-time analysis. Compared with traditional methods of single-cell analysis, Raman spectroscopy offers the incomparable advantages of label-free and noninvasive detection. At present, it is widely used to study the differences between malignant and normal cells.

Neoplastic cells characterized by cell atypia differ from normal cells not only in terms of their morphology but also in terms of their cellular behavior and biochemistry.[2] Investigations of their Raman spectra have revealed substantial differences, thus allowing these two types of cells to be successfully discriminated based on their intrinsic biomolecular signatures, especially when Raman spectroscopy is combined with statistical methods such as principal component analysis (PCA) and linear discriminant analysis (LDA).[3–5] This approach has been applied to human acute T-lymphocytic leukemia cells (JM-1), human acute T-lymphoblastic leukemia cells (Molt-4),[6] erythrocytes, leukocytes, acute myeloid leukemia cells (OCI-AML3), breast tumor cells,[7] and normal and sickle red blood cells.[8] In a Raman study of insulin-containing cells, Rong et al.[9] found that the spectrum of a single rat pancreatic β cell changes when the cell is stimulated with glucose. Hilderink et al.[10] investigated the tiny Raman spectral difference between a pancreatic β-cell line and an α-cell line, based on which human pancreatic β cells and α cells can be distinguished in whole-islet Raman imaging.

Insulinomas are the most common type of functioning islet cell tumor of the pancreas. As a rare disease, the prevalence of insulinoma is approximately 1/100,000 persons/year.[11] These tumors are typically small, single, benign, well circumscribed, and evenly distributed throughout the pancreas.[12] A functional tumor of this type secretes insulin in a manner that is not regulated by glucose, often causing low blood sugar levels (hypoglycemia), which may lead to symptoms such as anxiety, hunger, seizures, coma, and even death. Approximately 50% of such a tumor consists purely of β cells, whereas the remainder often contains α, δ, PP, and G-cells. With respect to their microcosmic morphologies, insulinoma cells are similar to normal β cells when evaluated under light microscopy and even electron microscopy.[11,13] These cells are all rich in mitochondria and endocrine insulin granules and display a rare mitotic figure. This similarity in cellular morphology remains an obstacle to differentiation for pathologists and researchers, especially *in vivo*. In actual clinical work, routine pathology techniques such as immunohistochemistry and even electron microscopy cannot distinguish between them.[14] Therefore, we hypothesize that based on the intrinsic biomacromolecular differences between these types of cells (such as their nucleic acid, protein and lipid contents), Raman spectroscopy can be used to discriminate between them based on the differences in their spectra. In this study, Raman spectroscopy was applied to a rat-origin INS-1 insulinoma cell line and to primary rat pancreatic β-cell populations *in vitro*, and the intrinsic differences between the cells were found to be detectable via their Raman spectra. Thus, Raman spectroscopy may be a promising method for distinguishing cells

*Address all correspondence to: Hong Liu, E-mail: hongmm1@qq.com

†These authors contributed equally to this work and should be considered co-first authors.

1083-3668/2015/$25.00

based on their biomolecular characteristics and a potential diagnostic tool for malignant insulinomas.

2 Experimental Methods

2.1 *Experimental Setup*

Near-infrared Raman spectroscopy has been described previously.[15] In brief, a wavelength-stabilized diode laser (HL-7851G, Hitachi, Japan) produced a laser beam (at a wavelength of 780 nm and a power of 20 mW), which was circularized by a pair of anamorphic prisms, spatially filtered, and then directed into an inverted differential interference contrast microscope (Nikon TE2000-U). This microscope was equipped with an objective (100×, numerical aperture of 1.30) to form an excitation source and a single-beam optical trap. The beam was focused through a quartz sample chamber with a thickness of 0.1 mm. For these experiments, we equipped a Focht Chamber System 2 (FCS2, Bioptechs), which is a closed-chamber system for live-cell observation, with a Raman system to ensure a constant temperature as well as perfusion of the culture medium and carbon dioxide which are beneficial for cell survival. Cells were grown in the FCS2 system and were probed by the laser. Raman-scattered light from the cells was collected by the objective, focused onto the entrance slit of an imaging spectrograph (Acton Research Co., SpectraPro 2300i, 600 lines/mm blazed at 650 nm) and recorded using a charge-coupled device (CCD, Roper Scientific Spec-10, Princeton Instruments). The resolution of the spectrograph was 6 cm^{-1}. A suspension of polystyrene beads (2 μm, Bands Laboratories) was used to calibrate the relative Raman shifts prior to each measurement.

2.2 *Pancreatic Islet Isolation and Single-Cell Acquisition*

Sprague–Dawley rats (8 to 10 weeks old, body weight 250 to 300 g, provided by the Guangxi Medical University Laboratory Animal Center) were sacrificed, and collagenase (Sigma) was injected into the ductal system for tissue digestion.[16] The tissue was dispersed under shaking after collagenase digestion. The islets were isolated through density-gradient centrifugation using Histopaque-1077 (Sigma). The islets were dispersed into single cells via trypsin (Sigma) digestion. The cells were plated and grown in culture dishes containing 40-mm-diameter coverslips overnight in Roswell Park Memorial Institute 1640 (RPMI 1640) culture medium (Invitrogen) supplemented with 10% (vol/vol) fetal calf serum, 100 IU/ml penicillin, 0.1 mg/ml streptomycin, and 5.6 mmol/l glucose, under environmental conditions of 37°C and 5% CO_2.

INS-1 insulinoma cells (from the Conservation Genetics Chinese Academy of Sciences Kunming Cell Bank, China, Kunming) were cultured in RPMI 1640 with 2.05 mmol/l L-glutamine (Invitrogen) supplemented with 10% fetal calf serum, 100 IU/ml penicillin, 0.1 mg/ml streptomycin, 2 mmol/l L-glutamine, 1 mmol/l sodium pyruvate, and 50 μmol/l b-mercaptoethanol (Sigma). Sterile conditions were maintained for all operations involving islet isolation and cell culture. All cells were attachment cultured in the FCS2 system.

2.3 *Collection of Raman Spectra*

Each circular coverslip (40 mm in diameter, Bioptechs) on which adherent cells were grown was transferred to the FCS2 system, which was mounted on a Nikon microscope equipped with a CCD camera and the Raman spectroscopy setup. After an image of the cells was acquired, the laser spot was repositioned onto three to four different regions within a cell to acquire a Raman signal for each of these cell regions to obtain the approximate overall information of the cell. The background spectra of the culture medium were acquired over the same scan area but in the absence of cells. The integration time (measurement time) for each cell was set to 30 s.

2.4 *Identification of Primary Pancreatic β Cells*

Primary pancreatic islets have been classically described as containing four different types of cells: insulin-producing β cells, glucagon-producing α cells, somatostatin-producing δ cells, and pancreatic-polypeptide-producing PP cells. To acquire the spectra of pure primary rat pancreatic β cells as contrast samples, we first detected the Raman spectra of the primary islet cells, and a series of photographs of each cell was acquired using a microscope. The relative positions of all detected cells were recorded. After Raman detection was complete, we fixed the cells with 4% (w/v) paraformaldehyde. Through staining via immunohistochemistry techniques (using an insulin antibody, as described below), the insulin-positive cells were determined to be β cells. Based on the relative positions of the positive cells, the β cells, whose Raman data had been previously obtained, were confirmed. The immunohistochemistry-negative cells were thus considered to be non-β cells, and their data were discarded.

2.5 *Immunohistochemistry Staining*

Slices with adherent cells were dried and fixed using paraformaldehyde and then washed three times with phosphate-buffered saline (PBS). The cell sections were then placed in 3% hydrogen peroxide (H_2O_2) for 10 min and washed three times with PBS. After being soaked in a permeabilization buffer (containing 0.4% Triton X-100) for 10 min and rinsed in PBS, all sections were incubated in 10% normal goat serum for 10 min and then incubated overnight in rabbit anti-insulin (H-86, diluted 1:200 in PBS, pH 7.4, 1% BSA, Santa Cruz Biotechnology, Inc.) in humidified chambers at 4°C. These sections were rinsed in PBS and incubated in biotinylated goat anti-rabbit IgG (Beijing Zhongshan Biotechnology Co., Ltd., China) diluted in PBS (pH 7.4, 1% BSA) in humidified chambers for 10 min at 37°C. The sections were rinsed again and incubated in enzyme tag chain mildew avidin horseradish (Beijing Zhongshan Biotechnology Co., Ltd., China) for 10 min in humidified chambers at 37°C. The sections were then rinsed again in PBS. The immunoreactivity was visualized by incubating the sections for 5 min in the chromogen 3,3-diaminobenzidine hydrochloride in the presence of 0.01% hydrogen peroxide. The sections were rinsed several times in tap water, and the dyed sections were then rinsed with hematoxylin for ~3 or 4 s, dehydrated through a graded series of ethanol solutions, and soaked in xylene. The slices were then dried at room temperature and sealed. Finally, the slices were observed under an optical microscope (Olympus BX 40, Japan); in the resulting images, positive particles appeared brown and negative particles appeared blue.

2.6 *Statistical Analysis*

Raman spectra were collected within the spectral region from 510 to 1800 cm^{-1}. This region corresponds to a molecular fingerprint region that contains most relevant biological fingerprints,

including those of disulfide bonds which are present in abundance in insulin. The cellular spectra of the different cell regions were averaged; other processes, including the subtraction of background spectra, intensity calibration, five-point smoothing, normalization and baseline calibration, were performed using Micro Origin 8.1 software. The Raman peak intensities (relative counts) were used as the measurement data and were processed using the SPSS 13.0 software package for Windows. Multivariate analysis of variance (MANOVA) was used to analyze the difference between the two cell types. Student's t-test was used to test the difference in each peak.[4] PCA was applied to all spectra to extract the major spectral features for individual cells. Subsequently, Fisher LDA, which is a standard linear technique for discriminant analysis, was applied to establish the separation between the rat pancreatic β cells and the INS-1 insulinoma cells.[17,18] P values of <0.05 were considered to be significant.

3 Results

3.1 *Raman Spectra of Pancreatic β Cells and Insulinoma Cells*

The Raman spectra of samples containing pancreatic β cells and insulinoma cells were acquired. The mean Raman spectrum of an insulinoma cell and that of a single pancreatic β cell are shown in Fig. 1(a). Figure 1(b) shows a single insulinoma cell under Raman spectroscopy, whereas Figs. 1(c) and 1(d) show three islet cells and their immunohistochemical staining, respectively, in the same optical section. A series of Raman peaks can be observed, including the vibration of the DNA backbone (785 cm^{-1}); phenylalanine (1002 cm^{-1}), C—C and C—H vibration modes associated with proteins and lipids (1445 cm^{-1}); and protein amide I-band vibrations (1655 cm^{-1}). The Raman spectrum of an individual cell includes contributions from all of its cellular components (nucleic acids, proteins, and lipids).

The MANOVA results indicate an overall significant difference between the two cell types ($P < 0.05$). With the spectra represented in the same coordinate system, as shown in Fig. 1(a), each main distinct Raman peak was employed for statistical testing using Student's t-test. The peaks at 562, 640, 725, 785, 852, 893, 937, 1003, 1053, 1175, 1320, 1337, 1605, 1615, and 1660 cm^{-1} exhibited significantly different mean intensities, as determined via t-test analysis ($P < 0.05$). The normalized intensities of the Raman peaks at 562, 640, 725, 852, 893, 937, 1002, 1175, 1605, 1615, and 1660 cm^{-1} were more intense for the pancreatic β cells than for the insulinoma cells, whereas the Raman bands at 785, 1053, 1320, and 1337 cm^{-1} exhibited higher intensities in the insulinoma cell samples. The specific assignments of individual peaks can be found in Table 1, and Fig. 2 shows the means and standard deviations of the significantly different peaks.

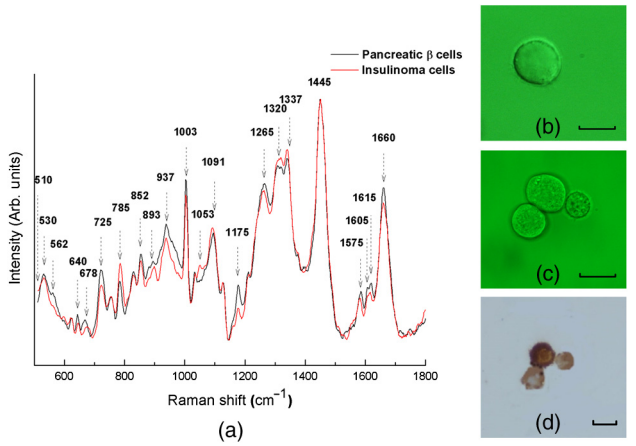

Fig. 1 (a) Comparison of the mean spectra for a pancreatic β cell (black line, $n = 60$) and an insulinoma cell (red line, $n = 77$); (b) insulinoma cell with the effect of differential interference contrast under the microscope; (c) three islet cells under the microscope; (d) immunohistochemical staining of the same three islet cells, only the middle of which appears immunohistochemistry-positive brown, indicating that it is a pancreatic β cell. The scale bars represent 10 μm.

3.2 *PC and LDAs of Raman Spectra*

Individual Raman spectra were analyzed via PCA to compress redundant spectral information and differentiate insulinomas from pancreatic β cells. Each spectral data set was imported into the SPSS software package for PCA and LDA. The PCA technique involves calculating the principal components (PCs) that describe the greatest proportion of the variance in the spectral data from its mean. Based on the PCA eigenvalues and the results of the PCA scree tests, 43 PCs were retained and calculated for LDA.

A three-dimensional (3-D) plot of the first principal component (PC1) versus the second principal component (PC2) and the third principal component (PC3) of the Raman spectra for the pancreatic β and insulinoma cells is shown in Fig. 3. PC1, PC2, and PC3 are responsible for 32.1%, 16.9%, and 9.6% of the variance, respectively. From Fig. 3, we can see that the two cell groups can be readily separated, thereby indicating inherent molecular differences between the cells, as a natural separation of the data is visible without supervised statistical manipulation.

The 43 PCs obtained from the PCA calculation were used as multivariate data for classification. Using the SPSS software package, the discriminant function was established via LDA and back-substitution tests of all cell spectra. The results are presented in Tables 2 and 3. Table 2 presents the classification results for the original cell data for which the discriminant algorithm was established based on all spectra; using this algorithm, each cell can be classified as a certain cell type. In the cross-validation, the discriminant algorithm was established using "leave one spectrum out" cross-validation. This involved removing one spectrum from the data set and constructing a diagnostic algorithm from the remaining spectra. The algorithm then predicted the cell type of the "left out" spectrum and stored the result. This process was repeated, with each spectrum left out in turn, until the cell type had been predicted for each of the spectra. The overall predictive accuracy of the algorithm was calculated and expressed in terms of sensitivity and specificity for each cell type. As shown in Table 2, there were 60 actual pancreatic β cells in total, of which 55 cells were correctly classified, whereas of the 77 total insulinoma cells, 76 cells were correctly classified; thus, the total accuracy was 95.6%. Similarly, Table 3 shows that 92.7% of the cross-validated grouped cases were correctly classified.

4 Discussion

An insulinoma is a type of pancreatic neuroendocrine tumor that is primarily derived from β cells and secretes insulin. Neuroendocrine tumors can be divided into two categories, nonfunctional and functional pancreatic neuroendocrine neoplasms

Table 1 Peak assignments for the Raman shifts of a pancreatic β cell.

Raman shift (cm^{-1})	Assignment[a]		
	DNA/RNA	Proteins	Lipids
510		S–S str	
640		C–C twist Tyr	
678	T, G		
725	A	Ring br Trp	C–N str
785	O–P–O str, C, T		
852		Ring br Tyr	
893	DNA bk/ deoxyribose		
937		Pro C–C bk	
1003		Sym ring br Phe	
1053	C–O str in deoxyribose	Pro C–N	
1091	DNA: O–P–O		Chain C–C str
1175		C–H in-plane bend Tyr	
1255		Amide III β sheet	=CH def
1320	G	Pro C–H def	
1337	A, G def		
1445		CH def	CH def
1575	A, G		
1605		C=C Phe, Tyr	
1615		C=C Tyr, Trp	
1660		Amide I α helix	C=C str

[a]Abbreviations: str, stretching; def, deformation vibration; sym, symmetric; br, breathing mode; bk, vibration of the DNA backbone; pro, protein; Phe, phenylalanine; Tyr, tyrosine; T, thymine; G, guanine; A, adenine; C, cytosine. Assignments are based on the results of previous studies.[19–22]

(NF-PNENs and F-PNENs). With their slow growth and low mitotic activity, NF-PNENs often exhibit a negligible clinical manifestation, whereas functional pNENs secrete insulin without regulation and cause hypoglycemia.

In rat insulinoma cells, the Raman peaks at 785, 1053, 1320, and 1337 cm^{-1}, which are attributed to the DNA backbone, deoxyribose and various nucleotides, are more intense than those of pancreatic β cells, which may indicate vigorous biosynthesis of nucleic acids within these cells, especially in the interphase of the

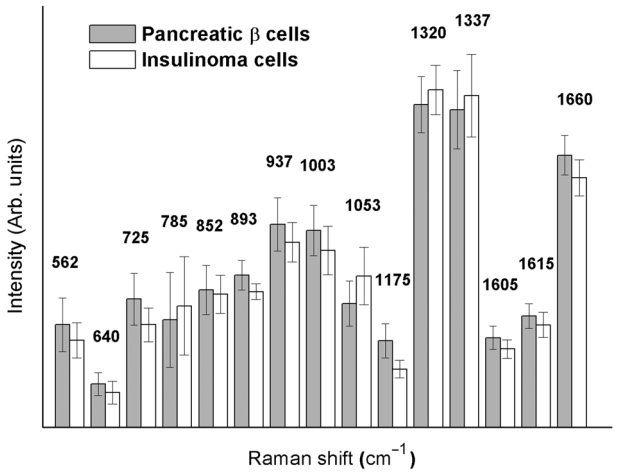

Fig. 2 The mean intensity values of significant peaks and the associated standard deviations for pancreatic β cells (gray) and insulinoma cells (white).

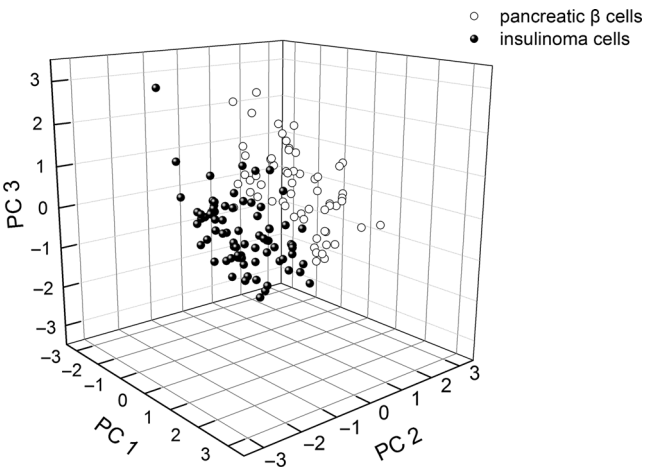

Fig. 3 A three-dimensional mapping of the PCA results for pancreatic β cells (white hollow balls) and insulinoma cells (black solid balls). PC1: the first principal component; PC2: the second principal component; and PC3: the third principal component.

cell cycle. However, the relative intensities of the peaks corresponding to proteins and amino acids at 640, 852, 893, 937, 1003, 1175, 1605, 1615, and 1660 cm^{-1} are lower, which indicates a lower protein concentration in tumor cells than that in β cells. The stronger peak at 725 cm^{-1} (attributed to adenine) in

Table 2 Classification results for the original cell data.

Cell	Prediction		
	Pancreatic β cell	Insulinoma	Total
Actual pancreatic β cell	55	5	60
Insulinoma	1	76	77
Percentage % pancreatic β cell	91.7	8.3	100
Insulinoma	1.3	98.7	100

Note: 95.6% of the original grouped cases were correctly classified.

Table 3 Classification results for the cross-validation test.

	Prediction		
Cell	Pancreatic β cell	Insulinoma	Total
Actual pancreatic β cell	52	8	60
Insulinoma	2	75	77
Percentage % pancreatic β cell	86.7	13.3	100
Insulinoma	2.6	97.4	100

Note: 92.7% of the cross-validated grouped cases were correctly classified.

pancreatic β cells may suggest an abundance of poly A or coenzyme A within these cells,[20] possibly indicating dynamic protein biosynthesis or energy metabolism in pancreatic β cells.

Several studies have reported the possibility of using Raman spectroscopy to differentiate cancer cells from their nonmalignant counterparts[23–25] as well as to discriminate cancer cells in different stages of differentiation.[26] Generally, because of tumor atypia such as larger nuclei, greater mitotic figures, and increased nuclear-to-cytoplasm ratios within malignant cells, the Raman spectra of malignant cells tend to express higher DNA/protein ratios in comparison with normal cells. This is consistent with the Student's *t*-test results obtained in this study.

The treatment of insulinoma frequently requires surgical operation. However, such tumors are often small and difficult to identify; insulinoma cells do not display overt cell atypia and are, therefore, difficult to recognize. Moreover, there are no distinguishing morphological features of pancreatic tumors that predict malignant properties, subsequent metastasis, or lymph node metastasis. Using traditional methods, pathologists cannot reliably distinguish these two types of cells under a microscope, especially *in vivo*. However, using Raman spectroscopy, subtle intrinsic differences can be detected. The use of PCA reduces the large amount of variability in the Raman spectra to a small number of important PCs. When this approach is applied, the pancreatic β cells and insulinoma cells form two clearly distinct clusters. In a 3-D scatter plot of PC1, PC2, and PC3, the pancreatic β cells and the insulinoma cells are distributed in clearly separated areas. The first three PCs (PC1, PC2, and PC3) can explain ~60% of the variance in a sample. The PCA–LDA method proposed in this study can be used to distinguish insulinoma cells from pancreatic β cells with a high rate of correct discrimination.

The primary limitation of Raman spectroscopy is its low detection speed; the analysis of a large number of cells using Raman spectroscopy is very time consuming. More work is required to further study the Raman spectral differences that are evident between insulinoma tissue and normal pancreas tissue *in vivo* and to extend its use from the analysis of tissue from intraoperative frozen sections to tumor diagnosis in human beings.

5 Conclusion

This study presents a preliminary analysis of the differences in the Raman spectra of animal insulinoma cells and primary pancreatic β cells. In this *in vitro* study, we measured the Raman spectra of rat insulinoma cells and primary rat pancreatic β cells via Raman spectroscopy and observed significant Raman spectral differences. The specific biomolecular differences of insulinomas include a higher DNA concentration and a lower cellular protein concentration relative to pancreatic β cells; these differences are interpreted as arising from vigorous biosynthesis of nucleic acid in the interphase of the cell cycle and a lower protein content in comparison with pancreatic β cells. Combined with the PCA–LDA method, Raman spectroscopy can be employed to identify cells via their intrinsic cellular differences with a high rate of correct discrimination. These results indicate tremendous promise for the development of Raman spectroscopy as a tool for the noninvasive and label-free differentiation of insulinoma cells and normal pancreatic β cells.

Acknowledgments

This research was supported by the National Natural Science Foundation of China under Grant No. 31160189. We thank the Laboratory of Biophysics of Guangxi Academy of Sciences for providing the laboratory apparatus, including the Raman spectroscopy setup.

References

1. J. Chan et al., "Raman spectroscopy and microscopy of individual cells and cellular components," *Laser Photonics Rev.* **2**(5), 325–349 (2008).
2. J. W. Chan, "Recent advances in laser tweezers Raman spectroscopy (LTRS) for label-free analysis of single cells," *J. Biophotonics* **6**(1), 36–48 (2013).
3. J. W. Chan et al., "Nondestructive identification of individual leukemia cells by laser trapping Raman spectroscopy," *Anal. Chem.* **80**(6), 2180–2187 (2008).
4. J. W. Chan et al., "Micro-Raman spectroscopy detects individual neoplastic and normal hematopoietic cells," *Biophys. J.* **90**(2), 648–656 (2006).
5. C. A. Owen et al., "Progress in Raman spectroscopy in the fields of tissue engineering, diagnostics and toxicological testing," *J. Mater. Sci. Mater. Med.* **17**(11), 1019–1023 (2006).
6. A. Y. Lau, L. P. Lee, and J. W. Chan, "An integrated optofluidic platform for Raman-activated cell sorting," *Lab Chip* **8**(7), 1116–1120 (2008).
7. S. Dochow et al., "Tumour cell identification by means of Raman spectroscopy in combination with optical traps and microfluidic environments," *Lab Chip* **11**(8), 1484–1490 (2011).
8. R. Liu et al., "Novel single-cell functional analysis of red blood cells using laser tweezers Raman spectroscopy: application for sickle cell disease," *Exp. Hematol.* **41**(7), 656–661 (2013).
9. X. Rong et al., "Real-time detection of single-living pancreatic beta-cell by laser tweezers Raman spectroscopy: high glucose stimulation," *Biopolymers* **93**(7), 587–594 (2010).
10. J. Hilderink et al., "Label-free detection of insulin and glucagon within human islets of Langerhans using Raman spectroscopy," *PLoS One* **8**(10), e78148 (2013).
11. P. Komminoth, P. U. Heitz, and J. Roth, "Human insulinomas: clinical, cellular, and molecular aspects," *Endocr. Pathol.* **10**(4), 269–281 (1999).
12. K. Vanderveen and C. Grant, "Insulinoma," *Cancer Treat. Res.* **153**(0), 235–252 (2010).
13. C. S. Grant, "Insulinoma," *Best Pract. Res. Clin. Gastroenterol.* **19**(5), 783–798 (2005).
14. B. Hirshberg et al., "Malignant insulinoma," *Cancer* **104**(2), 264–272 (2005).
15. H. L. Yao et al., "Raman spectroscopic analysis of apoptosis of single human gastric cancer cells," *Vib. Spectrosc.* **50**(2), 193–197 (2009).
16. S. Özcan, *Diabetes Mellitus: Methods and Protocols*, Humana Press, Totowa, New Jersey (2003).
17. P. Crow et al., "The use of Raman spectroscopy to differentiate between different prostatic adenocarcinoma cell lines," *Br. J. Cancer* **92**(12), 2166–2170 (2005).

18. T. Fearn, "Discriminant analysis," in *Handbook of Vibrational Spectroscopy*, J. M. Chalmers and P. R. Griffiths, Eds., pp. 2086–2093, Wiley, Chichester (2002).
19. I. Notingher, J. Selvakumaran, and L. L. Hench, "New detection system for toxic agents based on continuous spectroscopic monitoring of living cells," *Biosens. Bioelectron.* **20**(4), 780–789 (2004).
20. S. Feng et al., "Nasopharyngeal cancer detection based on blood plasma surface-enhanced Raman spectroscopy and multivariate analysis," *Biosens. Bioelectron.* **25**(11), 2414–2419 (2010).
21. N. Stone et al., "Near-infrared Raman spectroscopy for the classification of epithelial pre-cancers and cancers," *J. Raman Spectrosc.* **33**(7), 564–573 (2002).
22. I. Notingher et al., "Spectroscopic study of human lung epithelial cells (A549) in culture: living cells versus dead cells," *Biopolymers* **72**(4), 230–240 (2003).
23. M. V. Chowdary et al., "Discrimination of normal and malignant mucosal tissues of the colon by Raman spectroscopy," *Photomed. Laser Surg.* **25**(4), 269–274 (2007).
24. A. S. Haka et al., "In vivo margin assessment during partial mastectomy breast surgery using raman spectroscopy," *Cancer Res.* **66**(6), 3317–3322 (2006).
25. A. Nijssen et al., "Discriminating basal cell carcinoma from perilesional skin using high wave-number Raman spectroscopy," *J. Biomed. Opt.* **12**(3), 034004 (2007).
26. H. G. Schulze et al., "Assessing differentiation status of human embryonic stem cells noninvasively using Raman microspectroscopy," *Anal. Chem.* **82**(12), 5020–5027 (2010).

Qiu-li Zhou is a postgraduate student at Guangxi Medical University. Her adviser is professor Hong Liu. She has pursued research on the Raman spectra of pancreatic β cells for 7 years.

Xi Rong is an endocrinologist who works at the First Affiliated Hospital of Guangxi Medical University. He has pursued research on the Raman spectra of pancreatic β cells for 7 years.

Fang Wei is a postgraduate student at Guangxi Medical University. His adviser is professor Hong Liu. He has pursued research on the Raman spectra of pancreatic β cells for 7 years.

Rui-Qiong Luo is a postgraduate student at Guangxi Medical University. Her adviser is professor Hong Liu. She has pursued research on the Raman spectra of pancreatic β cells for 7 years.

Hong Liu is a professor of endocrinology at Guangxi Medical University and chief physician in the Department of Geriatric Endocrinology at the First Affiliated Hospital of Guangxi Medical University. She has pursued research on the Raman spectra of pancreatic β cells for 7 years.